Photonic microwave bandpass filter with improved dynamic range

Yu Yan and Jianping Yao*

Microwave Photonics Research Laboratory, School of Information Technology and Engineering, University of Ottawa, Ontario K1N 6N5, Canada
**Corresponding author: jpyao@site.uOttawa.ca*

Received April 7, 2008; revised June 15, 2008; accepted June 19, 2008; posted July 3, 2008 (Doc. ID 94741); published July 30, 2008

A technique to improve the dynamic range of a photonic microwave bandpass filter is proposed and experimentally demonstrated. The filter is implemented based on phase modulation to intensity modulation conversion using fiber Bragg gratings (FBGs) serving as frequency discriminators, with the optical carriers located at the left or right slopes of the FBGs, to generate positive or negative tap coefficients. The dynamic range of the photonic microwave bandpass filter is increased by reducing the optical-carrier-induced shot noise and relative intensity noise at the photodetector, which is realized by placing the optical carriers at the lower slopes of the FBG reflection spectra. A photonic microwave bandpass filter with an improvement in dynamic range of about 10 dB is demonstrated. © 2008 Optical Society of America

OCIS codes: 060.0060, 070.1170, 350.4010.

A photonic microwave filter is usually implemented based on an optical delay-line structure with a finite impulse response. Most of the efforts in the past few years are focused on the investigation of architectures to realize different functionalities, such as bandpass filtering with negative or complex coefficients. On the other hand, the performance of a photonic microwave filter should also be investigated. A key factor that limits the performance of a photonic microwave filter is the spurious-free dynamic range (SFDR) [1], defined as the difference between the minimum signal that can be detected above the noise floor and the maximum signal that can be filtered out without distortions.

It is known that the SFDR is limited by several noise sources, including the optical phase-induced intensity noise, shot noise, and relative intensity noise (RIN). For a photonic microwave filter that uses independent light sources with very narrow linewidth (several tens to hundreds of kilohertz), the phase-induced intensity noise is very small and can be neglected [2]. Therefore, the dominant noise sources are the shot noise and the RIN, both are associated with the average received optical power at the photodetector (PD). The powers of the shot noise and the RIN are linearly and quadratically proportional to the received optical power. Therefore, an effective solution to increase the SFDR is to reduce the average received optical power. The reduction of shot noise and the RIN to improve the dynamic range of a microwave-photonics link has been investigated recently, with different techniques being proposed, such as intensity-noise cancellation [3], optical carrier filtering [4], low biasing of a Mach–Zehnder modulator (MZM) [5,6], coherent detection [7], class-AB modulation [8], and optical phase modulation to intensity modulation (PM-IM) conversion using a fiber-Bragg-grating (FBG)-based frequency discriminator [9]. However, to our knowledge these techniques have not been applied to improve the dynamic range of a photonic microwave filter.

In this Letter, we demonstrate a technique to improve the dynamic range of a photonic microwave bandpass filter. The photonic microwave bandpass filter is implemented based on PM-IM conversion using FBGs as frequency discriminators, with the optical carriers located at the left or right slopes of the FBGs, to generate positive or negative coefficients. The dynamic range of the photonic microwave bandpass filter is increased by reducing the optical-carrier-induced shot noise and the RIN at the PD, by locating the optical carriers closer to the bottoms of the FBG reflection spectra. Although the technique using PM-IM conversion to generate negative coefficients for microwave bandpass filtering has been demonstrated by us [10–12], the implementation of the filter with an improved dynamic range has not been reported to our knowledge. With this technique, we demonstrate experimentally that a photonic microwave bandpass filter with an improvement in dynamic range of about 10 dB can be achieved.

The schematic diagram illustrating a two-tap photonic microwave filter is shown in Fig. 1. The output lightwaves from two independent tunable laser sources (TLSs) operating at different wavelengths are amplified by an erbium-doped fiber amplifier (EDFA), and then modulated by an rf signal to be filtered through an electro-optic phase modulator (EOPM). Two polarization controllers (PC1 and PC2)

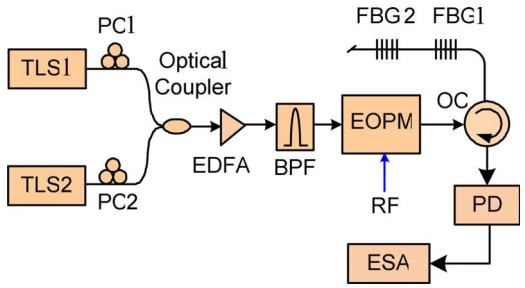

Fig. 1. (Color online) Photonic microwave bandpass filter. ESA, electrical spectrum analyzer; OC, optical circulator. Other abbreviations are defined in text.

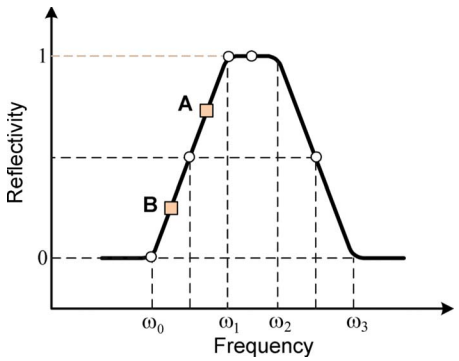

Fig. 2. (Color online) Reflection spectrum of an ideal FBG.

are connected between the TLSs and the EOPM to minimize the polarization-dependent loss. The rf signal carried by the two wavelengths is then time delayed by two cascaded FBGs to introduce a time-delay difference. Figure 2 shows the magnitude frequency response of an ideal FBG.

For a conventional photonic microwave filter, the optical carriers are usually tuned to locate at the center of the FBG reflection spectra. However, it is known that the shot noise at the PD exhibits a linear dependence on the average received optical power:

$$n_s = 2qI_0B, \tag{1}$$

where n_s (A^2) is the shot noise, q (A/Hz) is the unit electrical charge, I_0 (A) is the average detected photocurrent, and B (Hz) is the noise bandwidth.

Another noise source is the RIN, which exhibits a quadratic dependence on the average received optical power at the PD:

$$n_{\mathrm{RIN}} = I_0^2B(\mathrm{RIN}), \tag{2}$$

where n_{RIN} (A^2) is the RIN noise and RIN (Hz^{-1}) is the spectral power density of the intensity noise of a laser source. In addition, the use of an EDFA prior to the EOPM would add an amplified spontaneous emission (ASE) noise, which results from the beating between the rf signal and the ASE. The use of a narrowband optical filter after the EDFA, as shown in Fig. 1, would significantly reduce the ASE noise.

Obviously, if the received optical power is reduced, the powers of the shot noise and the RIN at the output of the PD will be reduced. The reduction of the received optical power can be achieved by tuning the wavelengths of the optical carriers away from the central reflection regions of the FBGs, as shown in Fig. 2. As the optical carrier wavelength is shifted from the top to a point closer to the bottom of the reflection spectrum, the shot noise is reduced linearly and the RIN falls quadratically. However, the reduction of the received optical power will also substantially decrease the rf signal power in an intensity-modulator-based system.

To increase the SFDR, it is highly desirable that the noise floor could be lowered without sacrificing much the signal power. This can be achieved by using the configuration shown in Fig. 1, where an EOPM is used. Mathematically, when a phase-modulated optical carrier ω_c is located at the left slope, the top, or the right slope of an FBG reflection spectrum, the recovered rf signal is [10]

$$r(t) \propto \begin{cases} K^2(\omega_c-\omega_0)^2 + 2K^2(\omega_c-\omega_0)\beta_{\mathrm{PM}}f'(t), & (\omega_0 < \omega_c < \omega_1) \\ 0, & (\omega_1 < \omega_c < \omega_2) \\ K^2(\omega_3-\omega_c)^2 - 2K^2(\omega_3-\omega_c)\beta_{\mathrm{PM}}f'(t), & (\omega_2 < \omega_c < \omega_3), \end{cases} \tag{3}$$

where K is the slope steepness of the FBG reflection spectrum; β_{PM} is the phase-modulation index, $f'(t)$ is the first-order derivative of the modulating signal; and ω_0, ω_1, ω_2, and ω_3 are the frequencies that define the frequency range of the left slope, the top, and the right slope of the FBG reflection spectrum, as shown in Fig. 2. The first and the second terms in Eq. (3) are respectively a dc and an ac component. Since the dc power decreases quadratically when the optical carrier is shifted closer to the bottom of the FBG spectrum while the signal power decreases linearly, the noise power is significantly decreased while maintaining a smaller decrease in the signal power. This important property enables us to choose a reflection point closer to the bottom of the FBG spectrum to substantially reduce the optical-power-induced noises with slightly sacrificing the signal power, leading to an increased SFDR. For example, in Fig. 2, if the optical carrier is shifted from A to B, the optical power is reduced by nine times, while the signal power is reduced by three times. Therefore, an improvement in SFDR of 5 dB is achieved.

In addition, when the optical carrier is located at one of the two slopes of the FBG spectrum, the FBG is acting as a frequency discriminator, to perform PM-IM conversion. Furthermore, for many applications microwave filters with bandpass functionality are highly desirable. It is seen from Eq. (3) that when the optical carrier is located at the positive or negative slope of the FBG spectrum, the amplitude of the recovered rf signal will have a positive or negative sign, which can be directly used to generate a positive or negative coefficient, to achieve bandpass functionality [11,12].

An experiment based on the configuration shown in Fig. 1 is performed. Two FBGs with central wavelengths of 1548.72 and 1549.61 nm are fabricated in hydrogen-loaded single-mode fiber. To investigate the improvement in dynamic range, we first replace the EOPM in Fig. 1 with an electro-optic intensity modulator (EOIM), and tune the wavelengths of the output lightwaves from the TLSs to locate exactly at the cen-

ters of the FBG spectra. Since the optical carriers are reflected at the tops of the FBG reflection spectra, high optical powers are obtained at the PD, leading to high noise powers. The power of one optical carrier at the PD is measured to be 0.6 dBm. The frequency response of the filter, shown in Fig. 3(a), is measured using a vector network analyzer (VNA, Agilent 8364A). As can be seen it is a lowpass filter with a free spectral range of 5.05 GHz. We then investigate the dynamic range of the lowpass filter. This is done by a two-tone test by applying two rf signals with frequencies at $f_1=5.01$ and $f_2=5.02$ GHz to the EOIM. Since the third-order distortions are the primary concern for the filters, we measure the third-order distortions at $2f_1-f_2=5$ and $2f_2-f_1=5.03$ GHz, as well as the noise floor (1 Hz bandwidth). The results are shown in Fig. 3(b). As can be seen, the noise floor is −150 dBm/Hz, and the third-order SFDR is 96.33 dB/Hz$^{2/3}$.

Then, the EOIM is replaced by an EOPM. We tune the optical wavelengths to 1548.58 and 1549.75 nm to locate at the left and the right slopes of the spectra of the FBGs, respectively. Thanks to the PM-IM conversion at the opposite slopes, a positive and a negative coefficient are generated. The filter is now a bandpass filter, with its frequency response shown in Fig. 4(a). The optical power at the PD is reduced to −7.8 dBm, so the optical-power-induced noises are substantially decreased, and the noise floor is reduced to −159 dBm/Hz. Again, a two-tone test is implemented, in which the input rf frequencies are chosen at $f_1=3.51$ and $f_2=3.52$ GHz. The third-order distortions are measured at $2f_1-f_2=3.5$ and $2f_2-f_1=3.53$ GHz. The measured third-order SFDR is 106.05 dB/Hz$^{2/3}$, and an improvement in dynamic range of about 10 dB is achieved.

By comparing the experimental results shown in Figs. 3 and 4, we find that the measured noise floor of the PM-IM-based bandpass filter is about 10 dB lower than that of the conventional EOIM-based lowpass filter. One may note that the measured rf signal power at the output of the PM-IM-based bandpass filter is actually higher than that at the output of the EOIM-based lowpass filter. The reason is that the phase-modulation efficiency is higher than that of the intensity modulation. That is to say, although the average optical power at the PD is higher using intensity modulation than using phase modulation, the output rf signal after the PM-IM conversion is stronger than that based on intensity modulation for the same optical carrier. By increasing the performance of the phase modulator and the linearity of the FBG reflection spectra, the modulation efficiency of the PM-IM conversion can be further increased.

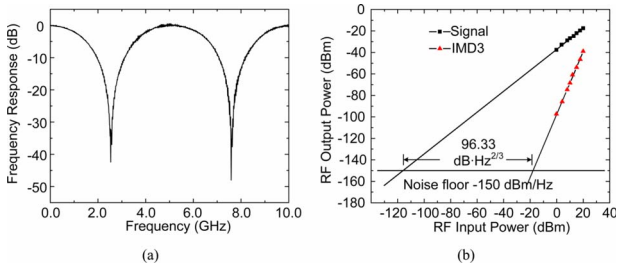

Fig. 3. (Color online) Dynamic range of a lowpass filter with the optical carriers located at the top of the FBG reflection spectra. (a) Frequency response, (b) dynamic range.

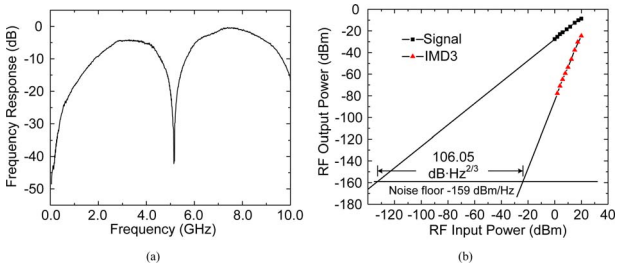

Fig. 4. (Color online) Dynamic range of a bandpass filter with the optical carriers located at the opposite slopes of the FBG reflection spectra. (a) Frequency response, (b) dynamic range.

In conclusion, a technique to increase the dynamic range of a photonic microwave bandpass filter was proposed and experimentally evaluated. The key to the technique was to lower the optical-carrier-induced noises to reduce the noise floor at the output of the filter. A better dynamic range was obtained when the optical carriers were located at the lower slopes of the FBG reflection spectra. One added advantage to the technique is that by locating the phase-modulated optical carriers at opposite slopes of the FBG reflection spectra, a microwave bandpass filter was obtained.

This work was supported by the Natural Sciences and Engineering Research Council of Canada (NSERC).

References

1. J. H. Schaffner and W. B. Bridges, J. Lightwave Technol. **11**, 3 (1993).
2. S. Yamamoto, N. Edagawa, H. Taga, Y. Yoshida, and H. Wakabayashi, J. Lightwave Technol. **8**, 1716 (1990).
3. S. Mathai, F. Cappelluti, T. Jung, D. Novak, R. B. Waterhouse, D. Siveco, A. Y. Cho, G. Ghione, and M. C. Wu, IEEE Trans. Microwave Theory Tech. **49**, 1956 (2001).
4. R. D. Esman and K. J. Williams, IEEE Photon. Technol. Lett. **7**, 218 (1995).
5. L. T. Nichols, K. J. Williams, and R. D. Esman, IEEE Trans. Microwave Theory Tech. **45**, 1384 (1997).
6. X. J. Meng and A. Karim, Fiber Integr. Opt. **25**, 161 (2006).
7. A. C. Lindsay, IEEE Trans. Microwave Theory Tech. **47**, 1194 (1999).
8. T. E. Darcie, A. Moye, P. F. Driessen, J. D. Bull, H. Kato, and N. A. F. Jaeger, in *International Topical Meeting on Microwave Photonics* (Seoul, South Korea, 2005), pp. 329–332.
9. J. Zhang and T. E. Darcie, in *Optical Fiber Communication Conference, and the National Fiber Optic Engineers Conference* (IEEE, 2006), paper OWG1.
10. Q. Wang and J. P. Yao, J. Lightwave Technol. **25**, 3626 (2007).
11. F. Zeng and J. P. Yao, Proc. SPIE **5971**, 59712B (2005).
12. J. Wang, F. Zeng, and J. P. Yao, IEEE Photon. Technol. Lett. **17**, 2176 (2005).